LA-UR-04- 5428

Approved for public release; distribution is unlimited.

Title: System Engineering Approach to GPM Retrieval Algorithms

Author(s): C. R. Rose
V. Chandrasekar

Submitted to: The 2nd TRMM International Science Conference

Los Alamos
NATIONAL LABORATORY

SYSTEM ENGINEERING APPROACH TO GPM RETRIEVAL ALGORITHMS

C. R. Rose* and V. Chandrasekar
Colorado State University

1. INTRODUCTION

System engineering principles and methods are very useful in large-scale complex systems for developing the engineering requirements from end-user needs. Integrating research into system engineering is a challenging task. The proposed Global Precipitation Mission (GPM) satellite will use a dual-wavelength precipitation radar to measure and map global precipitation with unprecedented accuracy, resolution and areal coverage. The satellite vehicle, precipitation radars, retrieval algorithms, and ground validation (GV) functions are all critical subsystems of the overall GPM system and each contributes to the success of the mission. Errors in the radar measurements and models can adversely affect the retrieved output values. Ground validation (GV) systems are intended to provide timely feedback to the satellite and retrieval algorithms based on measured data. These GV sites will consist of radars and DSD measurement systems and also have intrinsic constraints.

One of the retrieval algorithms being studied for use with GPM is the dual-wavelength DSD algorithm that does not use the surface reference technique (SRT). The underlying microphysics of precipitation structures and drop-size distributions (DSDs) dictate the types of models and retrieval algorithms that can be used to estimate precipitation. Many types of dual-wavelength algorithms have been studied. Meneghini (2002) analyzed the performance of single-pass dual-wavelength surface-reference-technique (SRT) based algorithms. Mardiana (2003) demonstrated that a dual-wavelength retrieval algorithm could be successfully used without the use of the SRT. It uses an iterative approach based on measured reflectivities at both wavelengths and complex microphysical models to estimate both *No* and *Do* at each range bin. More recently, Liao (2004) proposed a solution to the *Do* ambiguity problem in rain within the dual-wavelength algorithm and showed a possible melting layer model based on stratified spheres. With the *No* and *Do* calculated at each bin, the rain rate can then be calculated based on a suitable rain-rate model.

This paper develops a system engineering interface to the retrieval algorithms while remaining cognizant of system engineering issues so that it can be used to bridge the divide between algorithm physics and overall mission requirements. Additionally, in line with the systems approach, a methodology is developed such that the measurement requirements pass through the retrieval model and other subsystems and manifest themselves as measurement and other system constraints. A systems model has been developed for the retrieval algorithm that can be evaluated through system-analysis tools such as MATLAB/Simulink.

* *Corresponding author address:* C. R. Rose, Colorado State University, Dept of Electrical and Computer Engineering, Fort Collins, Colorado, 80523-1373. e-mail: chris.r.rose@colostate.edu

2. SYSTEM ENGINEERING APPROACH

One objective of system engineering is to maximize performance or output of a system while minimizing total costs or complexity. Figure 1 shows a simplified block diagram of some of the system-level interactions necessary to meet the GPM objectives.

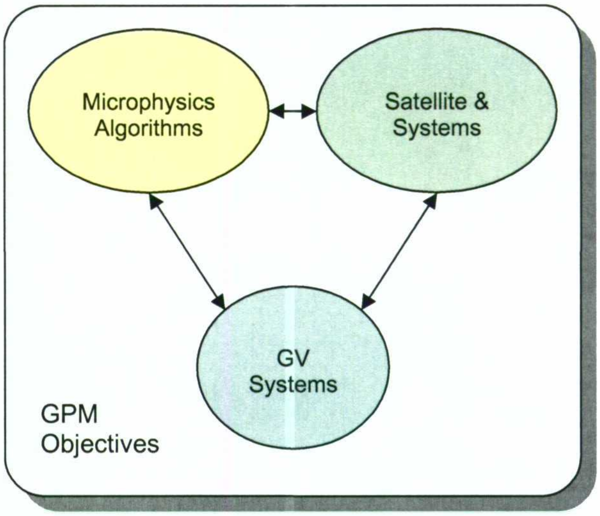

Figure 1. Simplified view of the interactions between the major GPM systems: Algorithms/microphysics; satellite and its subsystems; and the ground validation (GV) systems.

This is not meant to be inclusive but to show that algorithms and microphysics-based models are linked to both the GV and satellite systems. GV systems will have input to the algorithms and satellite systems. Each subsystem contributes, in conjunction with the other subsystems, to the overall success in meeting the GPM science objectives.

3. METHODOLOGY

Normally, to provide for a better systems engineering solution, it is necessary to understand the subsystems: how they perform; their strengths; their weaknesses; and how they interact with each other. The present work is beginning this process of complete systems understanding and is focused on the microphysics of the hydrometeors and the dual-wavelength algorithm.

3.1 ALGORITHM

The dual-wavelength algorithm iteratively solves for *Do* and *No* at each range bin based on microphysical models for each region of assumed hydrometeors: top; melting; and rain. A detailed explanation can be found in Mardiana (2003).

By way of brief summary, the measured radar reflectivity factor, *Zmi*, for each wavelength is given by

$$Zm_i(r) = Ze_i(r)\,A_i(r) \quad (1)$$

where the subscript i = 1 or 2 for wavelength one and two, $Ze_i(r)$ is the effective radar reflectivity factor and $A_i(r)$ is the total path-integrated attenuation (PIA).

$$Ze_i = N_o Ib_i(D_o(r)) \quad (2)$$

where

$$Ib_i = c_z \int_D \sigma_b(D,\lambda_2,\varepsilon_2) D^{\mu} e^{-\Lambda D}\, dD \quad (3)$$

$$k_i = N_o\ It_i(D_o(r)) \quad (4)$$

$$It_i = c_k \int \sigma_t(D,\lambda,\varepsilon)\, D^{\mu} e^{-\Lambda D}\, dD \quad (5)$$

and σ_b is the back scatter coefficient, σ_t is the extinction coefficient, c_Z and c_K are constants.

The algorithm starts at the bottom bin and works upward by estimating *PIA* values, A_i, for each frequency, and using those values to correct measured reflectivity, Zm_i, to obtain the effective radar reflectivity factors, Ze_i. With the calculated Ze_i factors, the *Do* at each bin can be calculated using a δZe_i-*Do* look-up table. Integral equations are used to calculate *No* and specific attenuation, k_i at each bin. *No* is calculated using

$$N_o(r) = \frac{Zm_i(r)}{A_i(r)\ Ib_i(Do(r))} \quad (6)$$

3.2 CONTROL SYSTEM VIEW

The non-SRT dual-wavelength algorithm convergence process can be thought of in control system terms. A simple block diagram is shown in figure 2 where the feedback is comprised of a single loop on *PIA*. The algorithm calculates the specific attenuation at each bin based on estimated *No* and *Do* values, then uses the bin values for specific attenuation to calculate a *PIA* value. That calculated *PIA* value is compared to the original value used at the start of the backward iteration. The error between the calculated and assumed start value is integrated and a new start value is calculated and used for the next iteration. This process is showed as a unit delay.

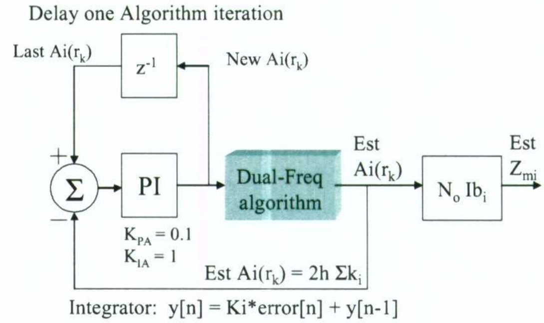

Figure 2. Block diagram of the dual-wavelength algorithm from a control systems perspective. A single loop operates as an integrator on the *PIA* variable for each wavelength.

Additionally, values for measured reflectivity can be calculated at each bin based on the calculated specific attenuation, *Do*, and *No* values and compared to the original, input Zm_i values. Given the fact that the algorithm operates as an integrator, an additional proportional-gain term can be added to decrease the number of iterations. Including a small gain of 0.1 for the proportional term has been shown to decrease the number of iterations for convergence while maintaining loop stability. The integrator gain term is unity.

The single-loop model can be expanded to include an additional, outer loop shown in figure 3 that may yield some improvements in reliability and efficiency. In this approach, the inner loop feeds back and converges on *PIA* and the outer loop converges on another variable such as Zm_i. In all cases, the algorithm converges and stops iterating by meeting a pre-defined error tolerance either on Zm_i or PIA_i.

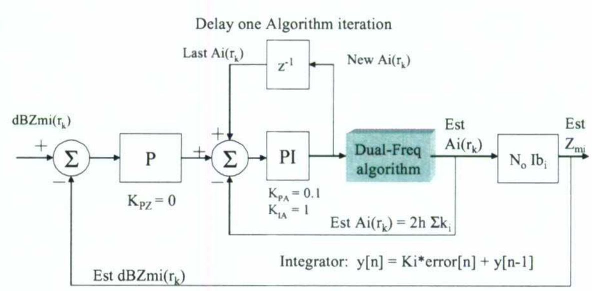

Figure 3. Simple feedback control system diagram of the dual-wavelength algorithm. The inner loop uses a PI control block and converges on PIA. The outer loop uses only a P block and converges on Zm_i.

Initially, with early simulations, single-loop convergence was done using Zm_i with no inner-loop feedback on *PIA*. However, when Zm_i converges, so do the PIA_i values, and a mathematically equivalent solution is to feedback and converge on PIA_i. As this is on-going work, the model presently only uses the inner loop on PIA_i

4. RESULTS

The algorithm has been successfully tested using simulations of known *Do* and *No* for regions of only rain and of rain/melting/snow. In each case, models were made for the δZe_i-*Do*, k_i and A_i relationships. Liao (2003) also made such models for the snow region.

An example of the rain output for synthesized *Do* = 1.50 mm, and *No* = 2041 is shown below in figure 4.

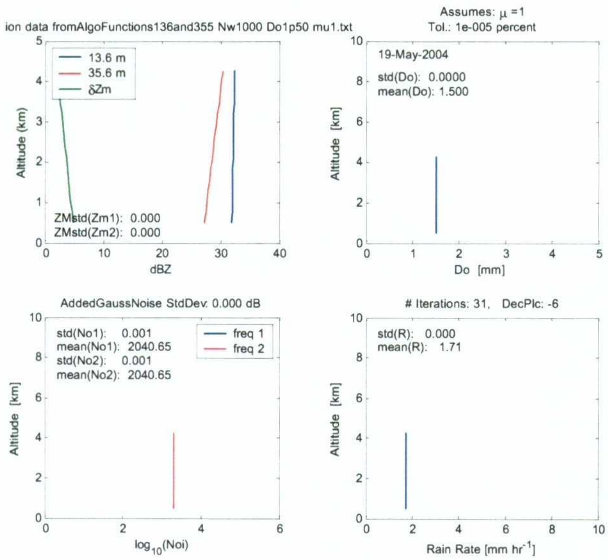

Figure 4 Plot showing how *Do* and *No* values are retrieved from synthesized *Zm*i values. Upper left: *Zm* values at 13.6 and 35.6 GHz. Upper right: retrieved *Do* values. Lower left: retrieved *No* values for both frequencies. Lower right: estimated rain rate based on *No* and *Do*.

The shape factor, μ, is equal to one. Many other *Do*/*No* combinations have been simulated and tested with the algorithm. It has been found that with certain combinations of *Do*/*No* that the algorithm converges but does not yield a straight vertical line for *Do* and *No* as it should. A chart of these solution regions is shown in figure 5.

The green diamonds are *Do*/*No* combinations that converge and yield unique solutions. The red asterisks are *Do*/*No* combinations that converge but do not yield unique solutions. With those simulated data sets, the *Do* and *No* retrieved values tend to curve at the bottom of the range.

5. SUMMARY

This paper has shown that a systems engineering approach requires a thorough understanding of the interactions of the various subsystems. For the GPM overall system, some of the key subsystems are: the satellite and its radar subsystems; the algorithms and microphysical assumptions; and the GV systems.

A model of the dual-wavelength algorithm has been presented that shows it operates with numerous assumptions including hydrometeor types and vertical regions. One of the most problematic regions is the melting layer. Additionally, the dual-wavelength algorithm can be viewed as a single or dual-loop control system with convergence on either *Zm* or *PIA*.

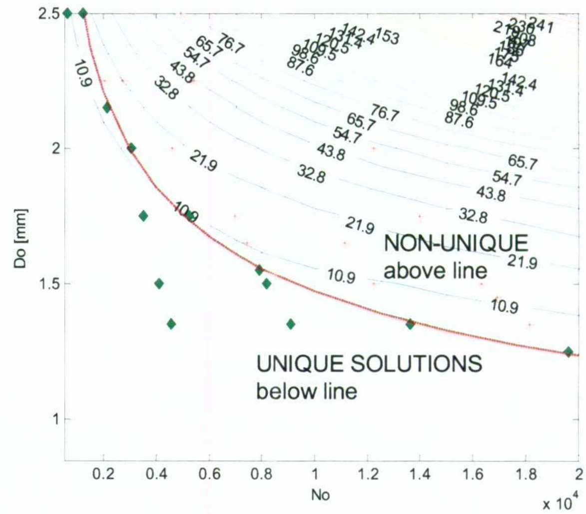

Figure 5. Contour plot of rain rate versus *Do* and *No*. Green diamonds represent *Do*/*No* combinations that have unique solutions. Red asterisks are *Do*/*No* combinations that converge but do not yield unique solutions. The solution boundary line is shown in heavy red.

Many reflectivity data sets, based on known *No*/*Do* combinations, have been simulated and tested with the algorithm. For the *No*/*Do* combinations below the unique solution boundary, the algorithm converges and retrieves the proper values. The specification of the convergence zones is being studied and will be reported in the future.

6. ACKNOWLEDGEMENTS

This research is jointly supported by the NASA Precipitation Program and Los Alamos National Laboratory.

References

Liao, L., R. Meneghini, 2004: On Study of Air/Space-borne Dual-Wavelength Radar for Estimates of Rain Profiles. 3rd Int'l Ocean Atmos. Conf., Beijing, China.

Liao, L., et al., 2003: Validation of Snow Parameters as Derived from Dual-Wavelength Airborne Radar. 31st Int'l Conf. Radar Meteorology.

Mardiana, R., et al., 2003: Dual-Frequency Rain Profiling Method Without the Use of Surface Reference Technique, IGARSS03

Meneghini, R., et al., 2002: Integral Equations for a Dual-Wavelength Radar, IGARSS02.